Impact of Al2O3 on the Aggregation and Deposition of Graphene Oxide

ARTICLE *in* ENVIRONMENTAL SCIENCE & TECHNOLOGY · APRIL 2014

Impact Factor: 5.33 · DOI: 10.1021/es404996b · Source: PubMed

11 AUTHORS, INCLUDING:

Xuemei Ren
Chinese Academy of Sciences
46 PUBLICATIONS **1,843** CITATIONS
SEE PROFILE

Jiaxing Li
Chinese Academy of Sciences
103 PUBLICATIONS **4,496** CITATIONS
SEE PROFILE

Xiaoli Tan
Chinese Academy of Sciences
77 PUBLICATIONS **3,583** CITATIONS
SEE PROFILE

Guixia Zhao
National Institute for Materials Science
34 PUBLICATIONS **1,776** CITATIONS
SEE PROFILE

Environmental Science & Technology

Article

pubs.acs.org/est

Impact of Al_2O_3 on the Aggregation and Deposition of Graphene Oxide

Xuemei Ren,[†] Jiaxing Li,[†] Xiaoli Tan,[†] Weiqun Shi,[‡] Changlun Chen,[†] Dadong Shao,[†] Tao Wen,[†] Longfei Wang,[§] Guixia Zhao,[†] Guoping Sheng,[§] and Xiangke Wang[†,∥,*]

[†]Institute of Plasma Physics, Chinese Academy of Sciences, P.O. Box 1126, 230031, Hefei, P.R. China

[‡]Institute of High Energy Physics, Chinese Academy of Sciences, Beijing, 100049, P.R. China

[§]Department of Chemistry, University of Science & Technology of China, 230026, Hefei, P.R. China

[∥]Faculty of Engineering, King Abdulaziz University, Jeddah 21589, Saudi Arabia

Supporting Information

ABSTRACT: To assess the environmental behavior and impact of graphene oxide (GO) on living organisms more accurately, the aggregation of GO and its deposition on Al_2O_3 particles were systematically investigated using batch experiments across a wide range of solution chemistries. The results indicated that the aggregation of GO and its deposition on Al_2O_3 depended on the solution pH and the types and concentrations of electrolytes. $MgCl_2$ and $CaCl_2$ destabilized GO because of their effective charge screening and neutralization, and the presence of NaH_2PO_4 and poly(acrylic acid) (PAA) improved the stability of GO with the increase in pH values as a result of electrostatic interactions and steric repulsion. Specifically, the dissolution of Al_2O_3 contributed to GO aggregation at relatively low pH or high pH values. Results from this study provide critical information for predicting the fate of GO in aquatic-terrestrial transition zones, where aluminum (hydro)oxides are present.

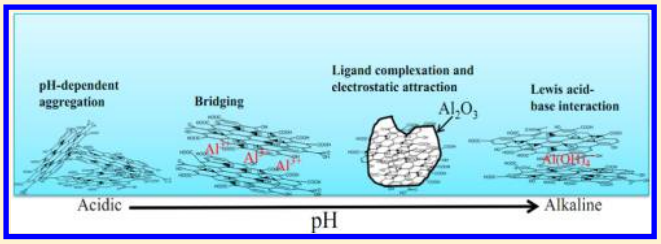

INTRODUCTION

Graphene oxide (GO) can serve as a substrate for many transformations, including the reduction to graphene-like materials,[1,2] the fabrication of graphene-based composites,[3] and the functionalization of graphene,[4,5] which dramatically increases the commercial synthesis and use of GO. The commercial market for graphene-related products is projected to be as large as $986.7 million by 2022.[6] With the widespread production and use of GO, it is inevitable that GO may be released into the environment as a contaminant during production, transport, use, and disposal processes. The potential risk of releasing GO into the environment will threaten human health and ecosystems.[7]

The toxicity of GO to various types of organisms has been demonstrated in recent studies. For example, GO caused cytotoxicity in human skin fibroblast cells and HeLa cells, in addition to dose-dependent hemolytic activity in human red blood cells.[8,9] GO exhibited high accumulation and long-term retention in mouse lungs, and a high dose of GO (GO: body weight = 10 mg: 1 kg) would cause remarkable pathological changes including pulmonary edema, inflammatory cell infiltration, and granuloma formation.[10] Once GO is released into the natural environment, the transport and retention processes will strongly affect its potential exposure pathways and bioavailability.[11] Therefore, thoroughly investigating the fate and transport of GO in the natural environment is of practical importance to minimize its negative environmental risk, in addition to protecting human health and ecosystems.

To date, a couple studies have been published on the aggregation kinetics and stability of GO over a broad range of aquatic solution chemistries,[12,13] and the results indicated that GO stability was independent of pH (4−10) and dependent on salt type and ionic strength. Two studies have been published on the transport of GO through porous media as investigated by performing column experiments,[14,15] and the results indicated that GO was increasingly mobile at low ionic strength. These results were crucial to understanding the behavior of GO in aquatic and subsurface environments. Natural solid particles are ubiquitous in aquatic-terrestrial transition zones, and the interactions between GO and these natural solid particles are likely to occur in addition to GO-GO interactions. One study has been published on the deposition of GO on a model mineral surface (silica), and it employed a quartz crystal microbalance.[16] However, no systematic studies have been conducted on the interaction between GO nanosheets and natural solid particles over a wide range of solution chemistries using batch experiments to more fully

Received: November 9, 2013
Revised: April 11, 2014
Accepted: April 22, 2014
Published: April 22, 2014

dx.doi.org/10.1021/es404996b | Environ. Sci. Technol. 2014, 48, 5493−5500

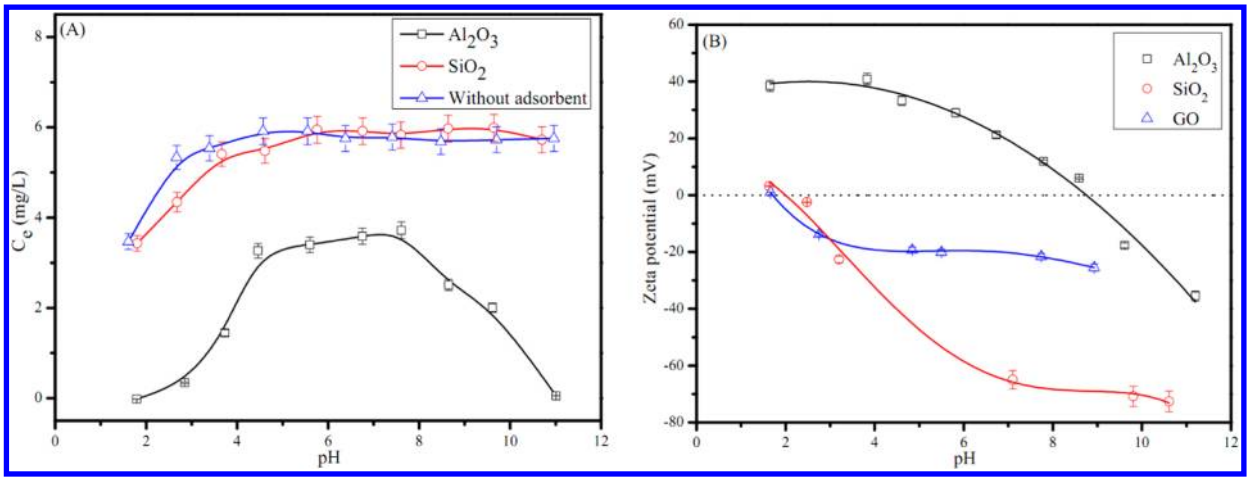

Figure 1. (A) Concentrations of the residual GO nanosheets in the supernatant as a function of pH in the absence and presence of natural particles (SiO_2 and Al_2O_3). $C_{(GO)initial}$ = 6 mg/L, m/V = 10 g/L (i.e., Al_2O_3 or SiO_2 concentration), I = 0.01 mol/L NaCl; (B) Zeta potentials of GO, Al_2O_3 and SiO_2 as a function of pH in the presence of 0.01 mol/L NaCl.

simulate the fate of GO nanosheets in aquatic-terrestrial transition zones.

In this study, Al_2O_3 was chosen as an representative natural solid particle because it can be used to model the layers of aluminum oxide in 1:1 clay minerals (e.g., kaolinite) and natural Al-hydroxide phases (e.g., gibbsite), which are commonly present in aquifers and soils.[17] By employing batch experiments, the aggregation and deposition of GO on Al_2O_3 was investigated across a wide range of solution chemistry conditions (including the pH, coexisting electrolyte (such as NaCl, $MgCl_2$, $CaCl_2$, Na_2SO_4 and NaH_2PO_4) concentrations, and poly(acrylic acid) (PAA)). Because little is known regarding the aggregation and deposition of GO in the presence of Al_2O_3, this study serves to identify potentially favorable and unfavorable conditions for the transport of GO in aquatic-terrestrial transition zones, where aluminum (hydro)-oxides are present. In addition, the dissolution behavior of Al_2O_3 in the absence and presence of GO were also investigated over a broad range of reaction times, which was expected to provide a brief outline of the potential impact of GO on oxide dissolution processes in the natural environment.

MATERIALS AND METHODS

Materials. All the chemicals (analytical grade) used in the experiments were purchased from Sinopharm Chemical Reagent Co. Ltd. (Shanghai, China). Al_2O_3 was purchased from Shanghai Ludu Chemical Reagents Factory (Shanghai, China). The Al_2O_3 size ranged from 74−300 μm. The natural flake graphite (with an average particle diameter of 20 mm and 99.95% purity) was obtained from Tianhe Graphite Co. Ltd. (Qingdao, China) and used to prepare GO by using the modified Hummers method. The detailed process was described in our previous study.[18] The resulting GO was dispersed in Milli-Q water to prepare a GO stock suspension (60 mg/L). The pH of the GO stock suspension was 5.8. The stock suspension had a dark brown color and was very stable even after 5 months of aging.[19]

Batch Experiments. The removal experiments were performed in a series of vials equipped with Teflon-lined screw caps by batch technique. A quantity of Al_2O_3 (0.1 g), GO stock suspension and the stock solution of the black electrolytes (NaCl, $MgCl_2$, $CaCl_2$, Na_2SO_4, or NaH_2PO_4) and PAA were added to the vials to achieve the desired concentrations of different components. The desired initial pH values (1.6−11.0) of the suspension in each vial were adjusted by adding negligible amounts of 0.1 mol/L NaOH or HCl. The removal experiments were performed as a function of the electrolyte concentrations by taking different concentrations of electrolytes at a fixed initial pH (5.50 ± 0.05). The vials containing these mixtures were placed on a horizontal shaker and shaken at a constant speed of 120 rpm for 24 h. Subsequently, the vials were removed from the shaker and left undisturbed on a flat surface for 24 h to allow for the complete settlement of Al_2O_3 and the large GO aggregates. Finally, the residual GO concentrations in the supernatant (C_e (mg/L)) were determined by UV-vis spectrophotometer (UV-2550, PerkinElmer) at a wavelength of 227 nm (SI Figure S1). In the Al_2O_3 solubility tests, filtration was performed with 0.22 μm membrane filters to remove GO from the supernatant. The Al(III) concentrations that were dissolved in solution were determined by an inductively coupled plasma-atomic absorption spectrometer (ICP-AAS, PerkinElmer). All the experimental data were averages of duplicate determinations, and the relative errors were approximately 5%.

Characterization. The zeta potentials of the samples were recorded as a function of the pH and the black electrolyte concentrations by using a Nanosizer ZS instrument (Malvern Instrument Co., UK) at 25 °C. The Al_2O_3 remaining after GO adsorption was rinsed with Milli-Q water several times, air-dried, and then used for image measurement by scanning electron microscopy (SEM). The SEM images were recorded on a field-emission scanning electron microscope (FEI Quanta 200 FEG SEM).

RESULTS AND DISCUSSION

pH Effect. Figure 1A presents the residual GO concentration changes in the supernatant (C_e) as a function of the pH (pH 1.6−11.0) in the absence and presence of natural solid particles (Al_2O_3 and SiO_2). The zeta potential data for GO, SiO_2, and Al_2O_3 at the different pH values are presented in Figure 1B. The extreme pH values were included to elucidate the roles of electrostatic interactions and the Al dissolution of Al_2O_3. As shown in Figure 1A, the C_e changes in the presence of SiO_2 were similar to those of C_e in the absence of SiO_2 or

dx.doi.org/10.1021/es404996b | Environ. Sci. Technol. 2014, 48, 5493−5500

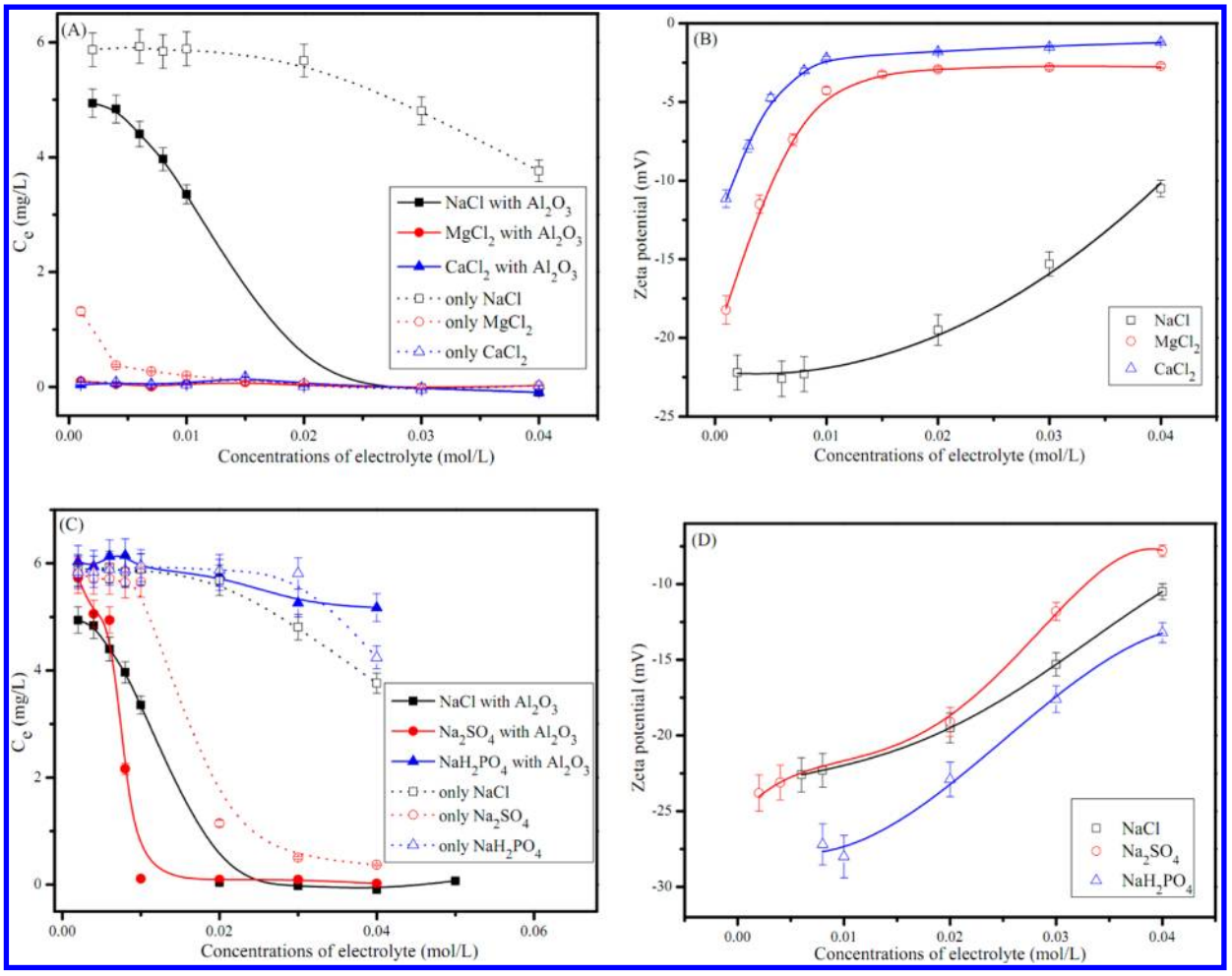

Figure 2. (A) Concentrations of the residual GO nanosheets in the supernatant as a function of cation types and concentrations in the absence and presence of Al_2O_3. $C_{(GO)initial}$ = 6 mg/L, m/V = 10 g/L (i.e., Al_2O_3 concentration), pH 5.50 ± 0.05; (B) Zeta potentials of GO as a function of cation types and concentrations at pH 5.50 ± 0.05. (C) Concentrations of the residual GO nanosheets in the supernatant as a function of anion types and concentrations in the absence and presence of Al_2O_3. $C_{(GO)initial}$ = 6 mg/L, m/V = 10 g/L (i.e., Al_2O_3 concentration), pH 5.50 ± 0.05; (D) Zeta potentials of GO as a function of anion types and concentrations at pH 5.50 ± 0.05.

Al_2O_3 at different pH values, and they were different from those of C_e in the presence of Al_2O_3. Figure 1A also shows that the C_e values in the presence of Al_2O_3 were much lower than the C_e in the presence of SiO_2.These results suggested that the pH and the nature of the solid particles played important roles in the aggregation and deposition of GO in aqueous solutions. SiO_2 with a pH_{PZC} (point of zero charge) value of ~2.0 (Figure 1B) has a lower efficiency in GO deposition than Al_2O_3 with a pH_{PZC} value of ~8.7 because of the strong electrostatic repulsion between the negatively charged SiO_2 and GO. In the absence of Al_2O_3 and SiO_2, the concentrations of residual GO nanosheets in the supernatant were only controlled by their pH-dependent colloidal stability.

As the pH values decreased from 4.5 to 1.6, the carboxyl groups that were presumably located at the edges of the GO nanosheets were increasingly protonated, which resulted in GO nanosheets becoming less hydrophilic and forming more aggregates.[20] When the GO nanosheets were exposed to Al_2O_3 in this pH range, ligand complexation and electrostatic attraction occurred.[21,22] During the interaction between GO and Al_2O_3, we observed an increase in pH values (SI Table S1) caused by the release of the hydroxyl ions, which was taken as direct evidence for the ligand complexation occurring through an exchange between the oxygen-containing groups of GO and the surface functional groups of Al_2O_3.[23] At the same time, the alumina was partially dissolved to generate Al^{3+} ions in this pH range (SI Figures S2 and S3). Many studies have shown that GO nanosheets had high adsorption capacities in the preconcentration and solidification of metal ions, such as Cd(II),[18] Co(II),[18] Pb(II),[19] and U(VI).[24] Therefore, one can deduce that GO can also strongly adsorb Al^{3+} ions when the pH is not extremely low. On one hand, the adsorption of Al^{3+} to GO would decrease the net negative surface charge of GO nanosheets, leading to a decrease in the GO stability. On the other hand, Al^{3+} ions acted as cross-linkers between GO nanosheets in the aggregates that formed.[22] Thus, the pH-dependent aggregation of GO, the interaction of GO with Al_2O_3, and the Al_2O_3 dissolution contributed to the decreased GO mobility at this acidic pH.

At pH 4.5−7.6, the deposition of GO on Al_2O_3 was primarily attributed to the interaction of GO with Al_2O_3 including ligand complexation and electrostatic interactions.[21,22,25] The SEM images (SI Figure S4) indicated that the Al_2O_3 surfaces changed from smooth to rough after GO adsorption. The distribution of GO on the Al_2O_3 surfaces was visually

dx.doi.org/10.1021/es404996b | Environ. Sci. Technol. 2014, 48, 5493−5500

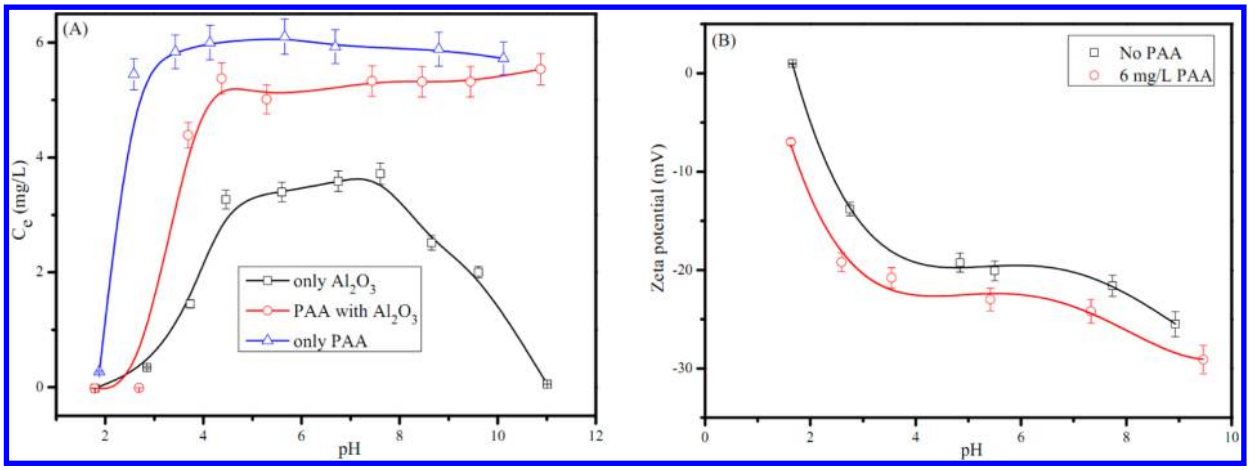

Figure 3. Effect of PAA on the concentrations of the residual GO nanosheeets in the supernatant at different pH in the absence and presence of Al_2O_3. $C_{(GO)initial}$ = 6 mg/L, C_{PAA} = 6 mg/L, m/V = 10 g/L (i.e., Al_2O_3 concentration), I = 0.01 mol/L NaCl. (B) Zeta potentials of GO as a function of pH in the absence and presence of 6 mg/L PAA.

inhomogeneous, and the coverage appeared to vary from one Al_2O_3 face to the other.

When GO nanosheets were exposed to Al_2O_3 at alkaline pH values (pH 7.6−11.0), more and more oxygen-containing functional groups on the surfaces of GO nanosheets were deprotonated, and the GO became more negatively charged and generated a stable aqueous suspension because of the electrostatic repulsion between negatively charged GO nanosheets. Further increasing the solution pH from 8.7 to 11.0 eliminated the positive surface charge of Al_2O_3 (Figure 1B), thereby creating an unfavorable condition for the deposition of GO nanosheets. The deposition of GO on Al_2O_3 should be unlikely because of the strong electrostatic repulsion between the negatively charged GO and Al_2O_3. However, the results of our batch experiments showed that the C_e values decreased with increasing pH values from 8.7 to 11.0. This finding was attributed to the Al dissolution of Al_2O_3 and the formation of $Al(OH)_4^-$ in aqueous solutions (SI Figures S2 and S3). As $Al(OH)_4^-$ is a Lewis acid, the delocalized π electron systems of the graphene layer as a Lewis base can form electron donor−acceptor complexes with $Al(OH)_4^-$.[18] A strong surface complexation between the GO nanosheets and $Al(OH)_4^-$ through the Lewis acid−base interaction contributed to the GO aggregation in aqueous solutions, and it therefore reduced the GO transport in the presence of Al_2O_3 at pH > 8.7.

Effect of Cation Types and Concentrations. The changes in C_e as a function of the cation types and concentrations in the absence and presence of Al_2O_3 were studied, and the results are illustrated in Figure 2A. The zeta potentials of GO as a function of NaCl, $MgCl_2$ and $CaCl_2$ concentrations were measured, and the results are presented in Figure 2B. Figure 2A shows that the values of C_e for all studied systems decreased with increasing ionic strength. The highest residual GO concentrations were found for the system without Al_2O_3 in the presence of 0.001−0.04 mol/L NaCl, and the lowest ones were found for the system with 10 g/L Al_2O_3 in the presence of 0.001−0.04 mol/L $CaCl_2$. These observations indicated that the cation types and the presence of Al_2O_3 played important roles in the aggregation and deposition of GO in the aqueous solutions, thereby affecting the fate and transport of GO in the environment.

The observed differences in the effects of bivalent cations (Mg^{2+} and Ca^{2+}) and monovalent cations (Na^+) on the aggregation and depositional behaviors of GO can be explained by the following: Bivalent cations with a higher valence provided better neutralization of the GO surface charge than monovalent cations at the same concentrations. This trend was evidenced by the finding that the presence of Mg^{2+} and/or Ca^{2+} was much more effective in increasing the zeta potential values of GO (Figure 2B) and decreasing the thickness of the electric double layer of GO. The latter was further supported by the formation of GO aggregates that were more compressed in the presence of 0.1 mol/L $CaCl_2$ than in the presence of 0.1 mol/L NaCl (SI Figure S5). Additionally, the Ca^{2+} ions showed a better binding capacity with oxygen-containing groups of GO than Mg^{2+} ions,[26] which resulted in a greater effect of Ca^{2+} ions on destabilizing GO than Mg^{2+} ions. The results from this study are consistent with those reported in previous publications.[12,13,16] It is worth noting that Wu and co-workers[13] also attributed a greater effect of Mg^{2+} and Ca^{2+} on destabilizing GO than Na^+ to the cross-linking between the functional groups at the edges of GO nanosheets by the divalent cations.

Effect of Anion Types and Concentrations. Figure 2C shows the C_e changes in the absence and presence of Al_2O_3 over a wide range of NaCl, Na_2SO_4 and NaH_2PO_4 concentrations at pH 5.50 ± 0.05. At pH 5.50 ± 0.05, the predominant phosphate and sulfate species were $H_2PO_4^-$ and SO_4^{2-}, respectively.[27,28] Figure 2D shows the effect of NaCl, Na_2SO_4, and NaH_2PO_4 concentrations on the zeta potential values of GO. One can see from Figure 2C that the C_e values varied as a function of the electrolyte concentrations. The variation was significant and depended on the types and concentrations of electrolytes in addition to the presence of Al_2O_3.

In the absence of Al_2O_3, the behaviors of the GO aggregation in the different electrolytes can be described as a balance between the anion (Cl^-, SO_4^{2-}, or $H_2PO_4^-$) and cation (Na^+) interfacial concentrations. On one hand, the adsorption of anions made GO more negative, which stabilized GO in aqueous solutions. On the other hand, the Na^+ concentrations increased with increasing electrolyte concentrations. The increased Na^+ concentrations were shown to increase the zeta potential of GO (Figure 2D) and thereby reduce their electrostatic repulsion, which then increased the aggregation of GO. The increased Na^+ had more pronounced effect on the colloidal properties of GO than the increased anion; thus, for a

dx.doi.org/10.1021/es404996b | Environ. Sci. Technol. 2014, 48, 5493−5500

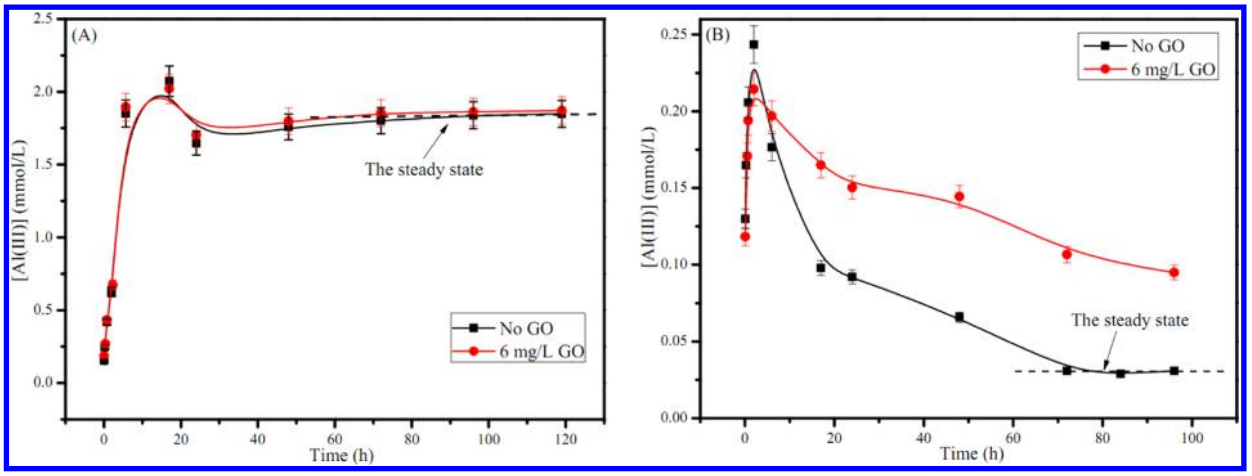

Figure 4. Concentrations of Al(III) dissolved from Al_2O_3 at pH 2.4 (A) and at pH 10.3 (B) as a function of shaking time in the absence and presence of GO. The Al_2O_3 concentration was 10 g/L and the background electrolyte was 0.01 mol/L NaCl in all cases. The initial concentration of GO was 6 mg/L. The scale of *y* axis is in range of 0.0−2.5 mmol/L for Figure 4A and 0.0−0.25 mmol/L for Figure 4B.

certain electrolyte (NaCl, Na_2SO_4, or NaH_2PO_4), the overall values of C_e decreased as the electrolyte concentration increased. Each mole of Na_2SO_4 contains two moles of Na^+ in comparison with only one mole for NaCl and NaH_2PO_4; thus, the presence of Na_2SO_4 induced a more pronounced aggregation of GO than the other two electrolytes at the high electrolyte concentration because of the charge screening and the compression of the electric double layer as caused by Na^+. In the presence of NaH_2PO_4, the strongly adsorbing anion ($H_2PO_4^-$)[29] could stabilize the GO in aqueous solutions because of the electrostatic repulsion and steric hindrance, and it consequently weakened the effectiveness of Na^+ in destabilizing GO. Therefore, the effect of the electrolytes on the GO aggregation in the absence of Al_2O_3 decreased in the following order: Na_2SO_4 > NaCl > NaH_2PO_4. The presence of Al_2O_3 further scavenged the residual GO nanosheets in the supernatant, and thus decreased the mobility of GO in environmental media.

PAA Effect. Poly(acrylic acid) (PAA), a polymeric substance containing carboxylic groups and linear CH_2-CH_2 chains, has the simple structure and similar properties with the natural organic matters (NOMs), which are ubiquitous in natural water and soils.[30,31] Most of all, the presence of PAA did not disturb the GO concentration detection by the UV-vis spectrophotometer (SI Figure S6). Therefore, PAA was selected as a NOM surrogate to study its effect on the interaction between GO and Al_2O_3 under different pH values, and the results are presented in Figure 3A. One can see that the presence of PAA reduced the aggregation of GO and its deposition on Al_2O_3 dramatically at pH > 2.8. Three possible explanations could be proposed for the GO stabilization by PAA as follows: (1) both GO and PAA were deprotonated as the pH value increased, which was clear when the GO surface became more negatively charged after PAA was added (Figure 3B), and thus PAA competed with GO for the limited active adsorption sites on Al_2O_3 and Al(III) species originating from Al_2O_3 dissolution, resulting in a decrease in the aggregation and deposition of GO; (2) PAA consisted of a hydrophobic backbone (CH_2-CH_2) and hydrophilic functional groups (−COOH). PAA could be readily adsorbed onto the basal plane of GO via hydrophobic interactions and prevented GO nanosheets from getting close to each other because of the steric hindrance effect.[32] Additionally, the exposed carboxyl groups of PAA made the GO surface more hydrophilic and more negative (Figure 3B), leading to the increased stability of GO and, consequently, making it more mobile in aqueous solution; and (3) the adsorbed PAA on the basal plane of GO prevented the $Al(OH)_4^-$ from getting close to GO and thus destroyed the Lewis acid−base interaction of GO with $Al(OH)_4^-$ at pH 8.7−11.0, leading to a decreased GO aggregation. At pH ≤ 2.8, the carboxyl groups of GO and PAA were protonated and the GO nanosheets became less hydrophilic and formed aggregates.[20] Considering the abundance of NOMs and their very different properties in natural waters, NOMs may effectively alter the transport behavior of the GO nanosheets released into natural environment.[33]

Solubility Tests for Al_2O_3. To elucidate the effect of GO on the dissolution of Al_2O_3, the Al(III) concentrations released from Al_2O_3 in the absence and presence of GO were measured over a reaction time range of up to 119 h. Figures 4A and 4B show the dissolution curves of Al_2O_3 in the absence and presence of GO at pH 2.4 and pH 10.3, respectively. The resulting kinetic dissolution curves showed that the dissolution behavior of Al_2O_3 was highly dependent on the pH, which was further supported by the dissolved curves of Al_2O_3 at different pH values (SI Figure S2). When the solubility test was performed in the acidic solution (pH 2.4), it became clear that the concentrations of dissolved Al(III) in the absence and presence of GO both tended to increase with increasing reaction time, and they then decreased slightly until approaching steady state. This phenomenon was believed to be caused by the continuous regeneration of dissolution-active sites on the Al_2O_3 surface.[34,35] In the presence of GO, the concentrations of Al^{3+} in the supernatant were controlled by multiple factors, including the dissolution of Al_2O_3 ($0.5Al_2O_{3(s)} + 3H^+ \rightleftharpoons Al^{3+}$), the adsorption of Al^{3+} on the GO surface, and the regeneration of Al_2O_3. At the low pH (pH 2.4), the Al^{3+} ions were barely adsorbed on GO nanosheets, and therefore the presence of GO had no obvious effect on the dissolution processes of Al_2O_3 at pH 2.4 (Figure 4A). In this case, both systems reached steady state after approximately 72 h of reaction time.

In the alkaline solution (pH 10.3) without GO, the high total concentrations of Al(III) dissolved from Al_2O_3 were observed at the beginning of the tests; over a reaction time of 2 h, the

dx.doi.org/10.1021/es404996b | Environ. Sci. Technol. 2014, 48, 5493−5500

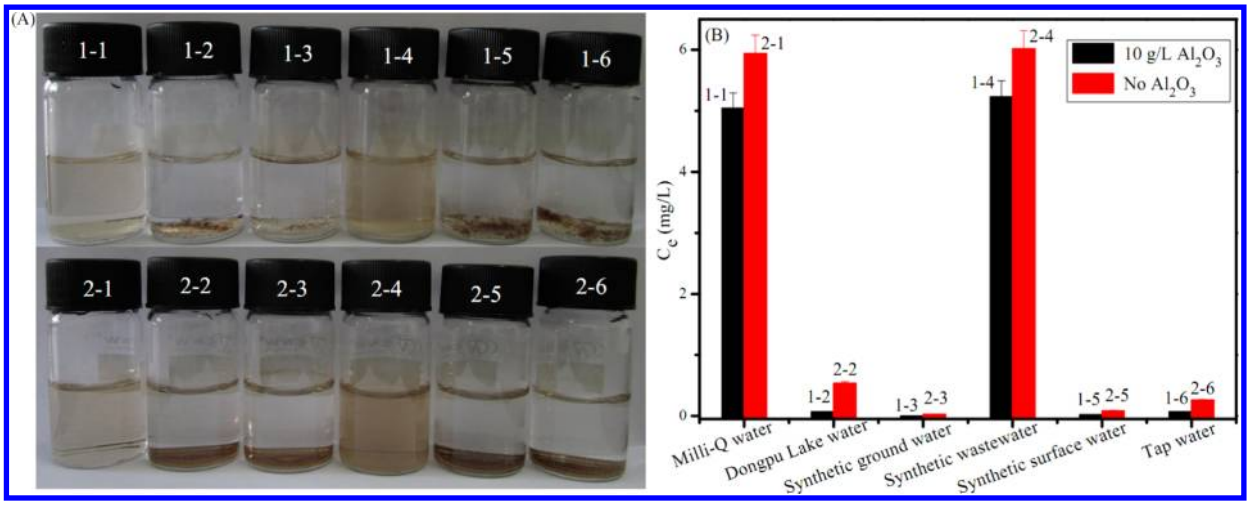

Figure 5. (A) Visual images of GO in the absence and presence of Al_2O_3 in different waters. (B) Concentrations of the residual GO nanosheets in the supernatant as a function of cation types and concentrations in the absence and presence of Al_2O_3 in the natural and synthetic waters. $C_{(GO)initial}$ = 6 mg/L, m/V = 10 g/L (i.e., Al_2O_3 concentration).

Al(III) concentrations decreased until they reached a constant value. Similar trends were also observed for Al dissolution from γ-Al_2O_3[36] and montmorillonite.[37] At pH 10.3, the dissolution of Al_2O_3 can be described as follows: $0.5Al_2O_{3(s)} + 1.5H_2O + OH^- \rightleftharpoons Al(OH)_4^-$. In the presence of GO, a strong surface complexation occurred between the GO nanosheets and $Al(OH)_4^-$ through the Lewis acid–base interaction, leading to a decrease in $Al(OH)_4^-$ concentrations in aqueous solution. Consequently, the reversible dissolution reaction mentioned above moved to the right, and more $Al(OH)_4^-$ ions were released from Al_2O_3 until a new equilibrium was attained. Here, the results showed that the dissolution process of Al_2O_3 did not reach the steady state even after 96 h of reaction time in the presence of GO at high pH values.

GO Stability in Natural and Synthetic Waters. Visual images of GO in the absence and presence of Al_2O_3 in different types of water are presented in Figure 5A. The C_e values in natural and synthetic waters are shown in Figure 5B. Details about the natural and synthetic waters are listed in SI. In the absence of Al_2O_3, the aggregation of GO was not observed in synthetic wastewater (conductivity 74 μS/cm, 100 mg/L total organic carbon (TOC)) and in Milli-Q water (conductivity 3.6 μS/cm), and the C_e values in these two systems were almost the same. The dissolved organic carbon in synthetic wastewater stabilized the GO and eliminated the effect of electrolytes on destabilizing GO nanosheets. When the GO nanosheets were in natural water, synthetic groundwater and synthetic surface water, they were settled down on the bottom of the bottle and the supernatants were nearly transparent. Because of the electronic layer compression and the charge screening and neutralization, the combined cations such as Na^+, K^+, Mg^{2+}, and Ca^{2+} in the synthetic ground (conductivity 220 μS/cm) and surface water (conductivity 75 μS/cm) destabilized GO nanosheets sufficiently. The NOMs in Dongpu Lake water and tap water were very low (3.7 ± 0.3 mg/L TOC for Dongpu Lake water and 3.1 ± 0.3 mg/L TOC for tap water) and cannot stabilize the GO nanosheets in solution. The aggregations of GO in Dongpu Lake water and in tap water were caused by their abundant electrolytes (with a conductivity of 105 μS/cm for Dongpu Lake water and 120 μS/cm for tap water). Undoubtedly, the results clearly demonstrate that the GO nanosheets are less likely to remain suspended and transported over long distances in the natural ground and surface water because of their abundant electrolytes. The Al_2O_3 further scavenged the residual GO nanosheets in the supernatant (Figure 5B), and thus decreased the mobility of GO in aquatic-terrestrial transition zones, where aluminum (hydro)oxides are present.

Environmental Implications. With the rapid production and broad applications of GO, its release into the environment is inevitable. Generally, the pH values of the aquatic environment range from 5.0–9.0.[12] Over these pH ranges, we observed no notable changes in the concentrations of residual GO nanosheets in the supernatant of systems without natural solid particles, suggesting that the pH values had minor effects on the fate and transport of GO in the natural aquatic environment. In the presence of Al_2O_3, the supernatant concentrations of GO significantly decreased. Therefore, the GO nanosheets are less likely to remain suspended and transported over long distances in the aquatic-terrestrial transition zones of environments, where kaolinite and gibbsite are present. The natural aquatic environment contains abundant electrolytes, and the various cations in the aquatic and soil environment usually range from 0.0001–0.02 mol/L,[38] which affects the surface charges of GO and the natural solid particles, and thus influences the aggregation of GO and its deposition on solid particles. Considering the abundance of NOMs in natural waters, these substances may effectively alter the transport behaviors of GO in the environment. However, these results showed that the NOM concentrations in natural water are not high enough to stabilize GO. As a result, the partition and deposition behaviors of GO in the environment are a complex function of many factors. GO may be much less stable and mobile in the natural environment than expected. These findings provide crucial insight regarding the fate and transport of GO in the natural environment and would partly allow us to assess its environmental impact.

■ ASSOCIATED CONTENT

Supporting Information

Seven figures (Figures S1–S7), two tables (Tables S1 and S2), and detailed descriptions of figures and tables can be found in the Supporting Information. This material is available free of charge via the Internet at http://pubs.acs.org.

AUTHOR INFORMATION

Corresponding Author

*Phone: +86-551-65592788; fax: +86-551-65591310; e-mail: xkwang@ipp.ac.cn.

Author Contributions

X.M.R. and J.X.L. contributed equally to this paper.

Notes

The authors declare no competing financial interest

ACKNOWLEDGMENTS

Financial support from 973 projects (2011CB933700), NSFC (21207136, 21307153, 41273134, 91326202, 21225730, 91126020) and Hefei Center for Physical Science and Technology (2012FXZY005), and open foundation of State Key Lab of Pollution Control and Resource Reuse are acknowledged.

REFERENCES

(1) Dreyer, D. R.; Park, S. J.; Bielawski, C. W.; Ruoff, R. S. The chemistry of graphene oxide. *Chem. Soc. Rev.* **2010**, *39* (1), 228−240.

(2) Gómez-Navarro, C.; Meyer, J. C.; Sundaram, R. S.; Chuvilin, A.; Kurasch, S.; Burghard, M.; Kern, K.; Kaiser, U. Atomic structure of reduced graphene oxide. *Nano Lett.* **2010**, *10* (4), 1144−1148.

(3) Thakur, S.; Das, G.; Raul, P. K.; Karak, N. Green one-step approach to prepare sulfur/reduced graphene oxide nanohybrid for effective mercury ions removal. *J. Phys. Chem. C* **2013**, *117* (15), 7636−7642.

(4) Bai, H.; Xu, Y. X.; Zhao, L.; Li, C.; Shi, G. Q. Non-covalent functionalization of graphene sheets by sulfonated polyaniline. *Chem. Commun.* **2009**, *13*, 1667−1669.

(5) Hsiao, M. C.; Liao, S. H.; Yen, M. Y.; Liu, P. I.; Pu, N. W.; Wang, C. A.; Ma, C. C. M. Preparation of covalently functionalized graphene using residual oxygen-containing functional groups. *ACS Appl. Mater. Interfaces* **2010**, *2* (11), 3092−3099.

(6) McWilliams, A. Graphene: Technologies, applications, and markets. *BCC Research, AVM075B* **2011**; http://www.bccresearch.com/market-research/advanced-materials/graphene-technologies-applications-markets-avm075b.html.

(7) Sanchez, V. C.; Jachak, A.; Hurt, R. H.; Kane, A. B. Biological interactions of graphene-family nanomaterials: An interdisciplinary review. *Chem. Res. Toxicol.* **2011**, *25* (1), 15−34.

(8) Liao, K. H.; Lin, Y. S.; Macosko, C. W.; Haynes, C. L. Cytotoxicity of graphene oxide and graphene in human erythrocytes and skin fibroblasts. *ACS Appl. Mater. Interfaces* **2011**, *3* (7), 2607−2615.

(9) Zhang, X. Y.; Hu, W. B.; Li, J.; Tao, L.; Wei, Y. A comparative study of cellular uptake and cytotoxicity of multi-walled carbon nanotubes, graphene oxide, and nanodiamond. *Toxicol. Res.* **2012**, *1* (1), 62−68.

(10) Zhang, X. Y.; Yin, J. L.; Peng, C.; Hu, W. Q.; Zhu, Z. Y.; Li, W. X.; Fan, C. H.; Huang, Q. Distribution and biocompatibility studies of graphene oxide in mice after intravenous administration. *Carbon* **2011**, *49* (3), 986−995.

(11) Li, Y. S.; Wang, Y. G.; Pennell, K. D.; Abriola, L. M. Investigation of the transport and deposition of fullerene (C_{60}) nanoparticles in quartz sands under varying flow conditions. *Environ. Sci. Technol.* **2008**, *42* (19), 7174−7180.

(12) Chowdhury, I.; Duch, M. C.; Manuskhani, N. D.; Hersam, M. C.; Bouchard, D. Colloidal properties and stability of graphene oxide nanomaterials in the aquatic environment. *Environ. Sci. Technol.* **2013**, *47* (12), 6288−6296.

(13) Wu, L.; Liu, L.; Gao, B.; Muñoz-Carpena, R.; Zhang, M.; Chen, H.; Zhou, Z. H.; Wang, H. Aggregation kinetics of graphene oxides in aqueous solutions: Experiments, mechanisms, and modeling. *Langmuir* **2013**, *29* (49), 15174−15181.

(14) Lanphere, J. D.; Luth, C. J.; Walker, S. L. Effects of solution chemistry on the transport of graphene oxide in saturated porous media. *Environ. Sci. Technol.* **2013**, *47* (9), 4255−4261.

(15) Feriancikova, L.; Xu, S. P. Deposition and remobilization of graphene oxide within saturated sand packs. *J. Hazard. Mater.* **2012**, *235*, 194−200.

(16) Chowdhury, I.; Duch, M. C.; Mansukhani, N. D.; Hersam, M. C.; Bouchard, D. Deposition and release of graphene oxide nanomaterials using a quartz crystal microbalance. *Environ. Sci. Technol.* **2014**, *48* (2), 961−969.

(17) Bargar, J. R.; Brown, G. E., Jr.; Parks, G. A. Surface complexation of Pb(II) at oxide-water interfaces: III. XAFS determination of Pb(II) and Pb(II)-chloro adsorption complexes on goethite and alumina. *Geochim. Cosmochim. Acta* **1998**, *62* (2), 193−207.

(18) Zhao, G. X.; Li, J. X.; Ren, X. M.; Chen, C. L.; Wang, X. K. Few-layered graphene oxide nanosheets as superior sorbents for heavy metal ion pollution management. *Environ. Sci. Technol.* **2011**, *45* (24), 10454−10462.

(19) Zhao, G. X.; Ren, X. M.; Gao, X.; Tan, X. L.; Li, J. X.; Chen, C. L.; Huang, Y. Y.; Wang, X. K. Removal of Pb(II) ions from aqueous solutions on few-layered graphene oxide nanosheets. *Dalton Trans.* **2011**, *40* (41), 10945−10952.

(20) Shih, C. J.; Lin, S. C.; Sharma, R.; Strano, M. S.; Blankschtein, D. Understanding the pH-dependent behavior of graphene oxide aqueous solutions: A comparative experimental and molecular dynamics simulation study. *Langmuir* **2012**, *28* (1), 235−241.

(21) Janot, N.; Reiller, P. E.; Zheng, X.; Croué, J. P.; Benedetti, M. F. Characterization of humic acid reactivity modifications due to adsorption onto α-Al_2O_3. *Water Res.* **2012**, *46* (3), 731−740.

(22) Shao, J. J.; Wu, S. D.; Zhang, S. B.; Lv, W.; Su, F. Y.; Yang, Q. H. Graphene oxide hydrogel at solid/liquid interface. *Chem. Commun.* **2011**, *47* (20), 5771−5773.

(23) Yang, K.; Lin, D. H.; Xing, B. S. Interactions of humic acid with nanosized inorganic oxides. *Langmuir* **2009**, *25* (6), 3571−3576.

(24) Zhao, G. X.; Wen, T.; Yang, X.; Yang, S. B.; Liao, J. L.; Hu, J.; Shao, D. D.; Wang, X. K. Preconcentration of U(VI) ions on few-layered graphene oxide nanosheets from aqueous solutions. *Dalton Trans.* **2012**, *41* (20), 6182−6188.

(25) Chen, K. L.; Elimelech, M. Interaction of fullerene (C_{60}) nanoparticles with humic acid and alginate coated silica surfaces: Measurements, mechanisms, and environmental implications. *Environ. Sci. Technol.* **2008**, *42* (20), 7607−7614.

(26) Nguyen, T. H.; Chen, K. L. Role of divalent cations in plasmid DNA adsorption to natural organic matter-coated silica surface. *Environ. Sci. Technol.* **2007**, *41* (15), 5370−5375.

(27) Ren, X. M.; Yang, S. T.; Tan, X. L.; Chen, C. L.; Sheng, G. D.; Wang, X. K. Mutual effects of copper and phosphate on their interaction with γ-Al_2O_3: Combined batch macroscopic experiments with DFT calculations. *J. Hazard. Mater.* **2012**, *237*−*238* (0), 199−208.

(28) Goh, K. H.; Lim, T. T. Influences of co-existing species on the sorption of toxic oxyanions from aqueous solution by nanocrystalline Mg/Al layered double hydroxide. *J. Hazard. Mater.* **2010**, *180* (1−3), 401−408.

(29) Boyle-Wight, E. J.; Katz, L. E.; Hayes, K. F. Macroscopic studies of the effects of selenate and selenite on cobalt sorption to γ-Al_2O_3. *Environ. Sci. Technol.* **2002**, *36* (6), 1212−1218.

(30) Yang, S. T.; Li, J. X.; Shao, D. D.; Hu, J.; Wang, X. K. Adsorption of Ni(II) on oxidized multi-walled carbon nanotubes: Effect of contact time, pH, foreign ions and PAA. *J. Hazard. Mater.* **2009**, *166* (1), 109−116.

(31) Chen, C. L.; Wang, X. K.; Nagatsu, M. Europium adsorption on multiwall carbon nanotube/iron oxide magnetic composite in the presence of polyacrylic acid. *Environ. Sci. Technol.* **2009**, *43* (7), 2362−2367.

(32) Xie, B.; Xu, Z. H.; Guo, W. H.; Li, Q. L. Impact of natural organic matter on the physicochemical properties of aqueous C_{60} nanoparticles. *Environ. Sci. Technol.* **2008**, *42* (8), 2853−2859.

(33) Mashayekhi, H.; Ghosh, S.; Du, P.; Xing, B. S. Effect of natural organic matter on aggregation behavior of C_{60} fullerene in water. *J. Colloid Interface Sci.* **2012**, *374*, 111−117.
(34) Hering, J. G.; Stumm, W. Fluorescence spectroscopic evidence for surface complex formation at the mineral - water interface: Elucidation of the mechanism of ligand-promoted dissolution. *Langmuir* **1991**, *7* (8), 1567−1570.
(35) Kraemer, S. M.; Hering, J. G. Influence of solution saturation state on the kinetics of ligand-controlled dissolution of oxide phases. *Geochim. Cosmochim. Acta* **1997**, *61* (14), 2855−2866.
(36) Roelofs, F.; Vogelsberger, W. Dissolution kinetics of nano-dispersed γ-alumina in aqueous solution at different pH: Unusual kinetic size effect and formation of a new phase. *J. Colloid Interface Sci.* **2006**, *303* (2), 450−459.
(37) Rozalen, M.; Huertas, F. J.; Brady, P. V. Experimental study of the effect of pH and temperature on the kinetics of montmorillonite dissolution. *Geochim. Cosmochim. Acta* **2009**, *73* (13), 3752−3766.
(38) Mukherjee, B.; Weaver, J. W. Aggregation and charge behavior of metallic and nonmetallic nanoparticles in the presence of competing similarly-charged inorganic ions. *Environ. Sci. Technol.* **2010**, *44* (9), 3332−3338.